Secrecy Analysis of PLC System with Channel Gain and Impulsive Noise

Vinay Mohan, Aashish Mathur, Vadde Aishwarya, and Shubham Bhargav
Department of Electrical Engineering
Indian Institute of Technology, Jodhpur, 342037, India
Email: {mohan.2, aashishmathur, aishwarya.1, bhargava.1}@iitj.ac.in

***Abstract*—Nowadays, modern world technologies are rapidly becoming part of the Internet of things (IoT) and 5G networks where the role of power line communication (PLC) technology will be predominant in some of the standard applications of IoT such as smart homes, smart industries, and smart grids by considering its favorable conditions. In this paper, we analyze the physical layer security (PLS) of a low-frequency PLC system in terms of average secrecy capacity (ASC), secure outage probability (SOP), and strictly positive secrecy capacity (SPSC) where the wiretap channel model is employed to measure the degree of data confidentiality between authorized and unauthorized user over low frequency PLC networks. The PLC channel characteristics are characterized by specifically, two different cases, when the main and wiretap channel are independent log-normally distributed and correlated log-normally distributed; concurrently the effect of impulsive noise is modeled by the Bernoulli Gaussian process. Furthermore, the impact of impulsive noise, the distance between the users, path loss factor, and transmitted power is also considered. The validity of the derived analytical results is established through close matching with the Monte Carlo based simulation results.**

***Index Terms*—Power line communication, physical layer security, average secrecy capacity, secure outage probability, strictly positive secrecy capacity, log-normal distribution, Bernoulli Gaussian.**

I. Introduction

POWER line communication is a kind of guided medium communication technology, in which we enable two-way digital communication over the electrical wires or power distribution network. In recent years, the revolution of IoT and 5G networks is changing the scenario of modern world technologies where many heterogeneous information and communication technologies are amalgamating with each other to make a complete smart optimized system. Among them, PLC can be a significant technology for IoT and 5G applications for instance, in smart homes, smart industries, and smart grids [1], [2]. The integration and conjunction of PLC with other technologies will be always advantageous in terms of reducing wiring infrastructure, the complexity of the system, robustness, reliability, capability of delivering high data rates, low cost, ubiquitous network connectivity throughout the home environment, cross-compatibility between wired and wireless for smart grid applications, and low-power network interfaces.

In the communication scenario, the security of data always has been an important concern for military as well as civilian applications. Especially in this modern, fast growing world, where huge number of users are interacting with each other via different technologies and applications, providing them an unbreachable communication security will always be a foremost matter for any communication technology. Recently, physical layer security (PLS) analysis in PLC has drawn the attention of researchers [3]-[4], where the PLS analysis is performed in terms of secrecy capacity. In [3], a comparative analysis of PLS performance has been performed among PLC and wireless channels in terms of secrecy rate and it is found that the secrecy rate in the PLC is low compared to wireless communications. PLS analysis has been carried out in [5] by considering a multi-input multi-output (MIMO) PLC system where it is shown that the secrecy capacity of a MIMO PLC system is more that of single input single output (SISO) PLC system. Further in [4], PLS of cooperative PLC networks is considered in the presence of passive eavesdropping.

In this work, we have inspected the PLS of a low-frequency PLC network by exploiting the channel characteristics of the main channel and wiretap channel. The total noise in the PLC channel is featured as a sum of background noise and impulsive noise; concurrently the effect of impulsive noise is characterized by the Bernoulli Gaussian process. The main contributions of this work are as follows:

1) Novel closed-form expressions of ASC, SOP, and SPSC for a low-frequency PLC system are derived contrary to[3] and [5] where explicit closed-form expressions are not available.
2) We have considered the effect of independent as well as correlated log-normally distributed PLC channels and Bernoulli Gaussian distributed PLC impulsive noise on the secrecy performance contrary to [3] and [5] where a different channel model and Gaussian noise model were used.
3) The effect of different parameters such as probabilistic occurrence of impulsive noise, path loss, transmitted power, and distance on ASC, SOP, and SPSC of the considered PLC system is comprehensively studied through which useful insights into the PLC secrecy performance can be obtained.

II. System Model

Let us consider a discrete memoryless power line wiretap channel shown in Fig. 1, where Alice (A) is a transmitter encoding the message and Bob (M) is a receiver decoding the received message. Both are legitimate users separated by

978-1-7281-1220-6/19/$31.00 ©2019 IEEE

a distance D_1 and forming the main channel. But, at the same time, their message could be tapped by an unauthorized user Eve (E) who is situated at a distance of D_2 from Alice (A) forming the wiretap channel.

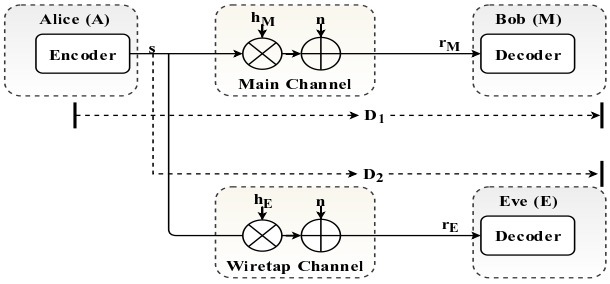

Fig. 1. Power line wiretap channel model

A. Received Power

The encoded message received by M and E is denoted by

$$r_M = \sqrt{P_{R_M}} h_M s + n, \tag{1-a}$$

$$r_E = \sqrt{P_{R_E}} h_E s + n, \tag{1-b}$$

where h_M and h_E are complex channel gains assumed to undergo flat fading [6], [7] and s denotes the single carrier modulated symbol, transmitted by A. The received power at the k^{th} node, $k \in (M, E)$ can be written as [8]

$$P_{R_k}(\text{dB}) = P_T(\text{dB}) - P_L(\text{dB/km}) \times D_k, \tag{2}$$

where P_L indicates the attenuation factor with distance in dB/km, P_T denotes the transmitted power (in dB), and D_k is the distance between A to k^{th} node, $k \in \{M, E\}$. The distance-dependent attenuation model is considered for low-frequency PLC networks [8], [9]. At such low frequencies, skin effect and dielectric losses can be neglected. The transmission path signal attenuation in PLC systems typically lies in the range of 40-100 dB/km [8]-[10].

B. PLC Channel Model

For the considered PLC system, we assume that both main and wiretap channel are independent log-normally distributed and correlated log-normally distributed. The probability density function (pdf) of the channel gain is expressed as

$$f\left(|h_k|; \mu_k, \sigma_k\right) = \frac{1}{|h_k|\sqrt{2\pi\sigma_k^2}} \exp\left(-\frac{\left(\ln|h_k| - \mu_k\right)^2}{2\sigma_k^2}\right), \quad k \in \{M,E\} \tag{3}$$

where μ_k and σ_k^2 are mean and variance, respectively, of the random variable $\ln|h_k|$ and $h_k \geq 0$.

C. Noise Modeling

The PLC channel noise is a combination of background noise and impulsive noise [11], [12]. The amplitude of impulsive noise rapidly varies at a very high rate which directly boosts the noise power by manifold. Hence, the total noise can be written as [12]

$$n = G_{n_1} + I_n, \tag{4-a}$$

$$I_n = P_B G_{n_2}, \tag{4-b}$$

where G_{n_1} and G_{n_2} denote Gaussian random variables with zero mean and variances σ_B^2 and σ_I^2. I_n represents impulsive noise which is modeled by Bernoulli Gaussian process. Eq. (4-b) describes the multiplicative model where the random amplitude of G_{n_2} affects each transmitted symbol independently and randomly according to Bernoulli random variable (P_B) with probability p. Moreover, G_{n_1}, G_{n_2}, and P_B are considered as mutually independent.

Thus, the pdf of PLC channel noise on both A to $M$and A to E links is given by [13]

$$f(n) = (1-p)\mathcal{CN}(0, \sigma_B^2) + p\mathcal{CN}(0, \sigma_B^2 + \sigma_I^2), \tag{5}$$

where $\mathcal{CN}(0, \sigma^2)$ indicates complex Gaussian distribution having zero mean and variance σ^2 and the arrival probability of impulsive noise samples is denoted by p.

The instantaneous signal-to-noise ratio (SNR) of the received signals at M and E can be written as [13]

$$\begin{aligned}\gamma_k &= \begin{cases} \gamma_{k_1} = \dfrac{|h_k|^2 P_{R_k}}{\sigma_B^2}, & \text{only background noise,} \\ \gamma_{k_2} = \dfrac{|h_k|^2 P_{R_k}}{\sigma_B^2(1+K)}, & \text{with impulsive noise,} \end{cases} \\ &= \begin{cases} \gamma_{k_1} = |h_k|^2 \overline{\gamma}, & \text{only background noise,} \\ \gamma_{k_2} = |h_k|^2 \overline{\gamma}', & \text{with impulsive noise,} \end{cases} \end{aligned} \tag{6}$$

where $k \in \{M, E\}$, $\overline{\gamma} = P_{R_k}/\sigma_B^2$, $\overline{\gamma}' = \overline{\gamma}/(K+1)$, and $K = \sigma_I^2/\sigma_B^2$. The pdf of the instantaneous SNRs for both the links are expressed as [13]

$$f_{\gamma_{k_1}}(\gamma) = \frac{1}{\gamma\sqrt{2\pi\sigma_{\gamma_{k_1}}^2}} \exp\left(-\frac{(\ln\gamma - \mu_{\gamma_{k_1}})^2}{2\sigma_{\gamma_{k_1}}^2}\right), \tag{7}$$

$$f_{\gamma_{k_2}}(\gamma) = \frac{1}{\gamma\sqrt{2\pi\sigma_{\gamma_{k_2}}^2}} \exp\left(-\frac{(\ln\gamma - \mu_{\gamma_{k_2}})^2}{2\sigma_{\gamma_k}^2}\right), \tag{8}$$

where $k \in \{M, E\}$, $\mu_{\gamma_{k_1}} = 2\mu_{h_k} + \ln\overline{\gamma}$, $\mu_{\gamma_{k_2}} = 2\mu_{h_k} + \ln\overline{\gamma}'$, and $\sigma_{\gamma_{k_1}}^2 = \sigma_{\gamma_{k_2}}^2 = 4\sigma_{h_k}^2$.

III. Physical Layer Security Analysis

In this section, we compute the PLS performance of the considered PLC system in terms of ASC, SOP, and SPSC.

A. Preliminaries

To simplify the mathematical derivation, some basic concepts have been applied in the analysis of ASC, SOP, and SPSC. Let $\Lambda(x)$ be a real function of x which is normally distributed with variables μ and σ, viz $X \sim N(\mu, \sigma^2)$. Then, the expectation of $\Lambda(x)$ upto three terms can be written as follows[14], [15]:

$$\mathbf{E}\left[\Lambda(x)\right] \approx \frac{2}{3}\Lambda(\mu) + \frac{1}{6}\Lambda\left(\mu + \sqrt{3}\sigma\right) + \frac{1}{6}\Lambda\left(\mu - \sqrt{3}\sigma\right), \tag{9}$$

where $\mathbf{E}[\cdot]$ denotes the expectation operator.

B. Computation of ASC

Secrecy capacity is a measure of amount of data that can be reliably and securely communicated between two parties without any leakage of data towards a third party. The instantaneous secrecy capacity, $\mathbf{C_s}$, for a wiretap channel can be realized [16] as follows:

$$\mathbf{C_s}(\gamma_M,\gamma_E)=\begin{cases}\log(1+\gamma_M)-\log(1+\gamma_E) & \text{if } \gamma_M>\gamma_E\\ 0 & \text{if } \gamma_M\leq\gamma_E.\end{cases} \tag{10}$$

1) *Case-I, Independent main and wiretap PLC channel:* The analytical ASC of the considered PLC system is given by

$$\begin{aligned}\bar{\mathbf{C}}_{\mathbf{s}}(\gamma_M,\gamma_E)&=(1-p)\times\mathbf{E}\left[\mathbf{C_s}(\gamma_{M_1},\gamma_{E_1})\right]\\&\quad+p\times\mathbf{E}\left[\mathbf{C_s}(\gamma_{M_2},\gamma_{E_2})\right]\\&=(1-p)\times\int_0^\infty\int_0^\infty\mathbf{C_s}(\gamma_{M_1},\gamma_{E_1})f(\gamma_{M_1},\gamma_{E_1})\,d\gamma_{M_1}\,d\gamma_{E_1}\\&\quad+p\times\int_0^\infty\int_0^\infty\mathbf{C_s}(\gamma_{E_2},\gamma_{E_2})f(\gamma_{E_2},\gamma_{E_2})\,d\gamma_{E_2}\,d\gamma_{E_2}\\&=(1-p)\times\left[\int_0^\infty\int_0^{\gamma_{M_1}}\mathbf{C_s}(\gamma_{M_1},\gamma_{E_1})f(\gamma_{M_1})f(\gamma_{E_1})d\gamma_{E_1}d\gamma_{M_1}\right.\\&\quad\left.+\int_0^\infty\int_{\gamma_{M_1}}^\infty\mathbf{C_s}(\gamma_{M_1},\gamma_{E_1})f(\gamma_{M_1})f(\gamma_{E_1})d\gamma_{E_1}d\gamma_{M_1}\right]\\&\quad+p\times\left[\int_0^\infty\int_0^{\gamma_{M_2}}\mathbf{C_s}(\gamma_{M_2},\gamma_{E_2})f(\gamma_{M_2})f(\gamma_{E_2})d\gamma_{E_2}d\gamma_{M_2}\right.\\&\quad\left.+\int_0^\infty\int_{\gamma_{M_2}}^\infty\mathbf{C_s}(\gamma_{M_2},\gamma_{E_2})f(\gamma_{M_2})f(\gamma_{E_2})d\gamma_{E_2}d\gamma_{M_2}\right]\\&=(1-p)\times\left[\int_0^\infty\ln(1+\gamma_{M_1})f(\gamma_{M_1})\int_0^{\gamma_{M_1}}f(\gamma_{E_1})d\gamma_{E_1}d\gamma_{M_1}\right.\\&\quad\left.-\int_0^\infty\ln(1+\gamma_{E_1})f(\gamma_{E_1})\int_{\gamma_{E_1}}^\infty f(\gamma_{M_1})d\gamma_{M_1}d\gamma_{E_1}\right]+\\&\quad p\times\left[\int_0^\infty\ln(1+\gamma_{M_2})f(\gamma_{M_2})\int_0^{\gamma_{M_2}}f(\gamma_{E_2})d\gamma_{E_2}d\gamma_{M_2}\right.\\&\quad\left.-\int_0^\infty\ln(1+\gamma_{E_2})f(\gamma_{E_2})\int_{\gamma_{E_2}}^\infty f(\gamma_{M_2})d\gamma_{M_2}d\gamma_{E_2}\right]\\&=(1-p)\times\left[\bar{\mathbf{C}}'_{M_1}(\gamma_{M_1})-\bar{\mathbf{C}}'_{E_1}(\gamma_{E_1})\right]\\&\quad+p\times\left[\bar{\mathbf{C}}'_{M_2}(\gamma_{M_2})-\bar{\mathbf{C}}'_{E_2}(\gamma_{E_2})\right].\end{aligned} \tag{11}$$

In (11),

$$\begin{aligned}\bar{\mathbf{C}}'_{M_j}(\gamma_{M_j})&=\int_0^\infty\ln(1+\gamma_{M_j})\mathbf{\Phi}\left(\frac{\ln\gamma_{M_j}-\mu_{\gamma_{E_j}}}{\sigma_{\gamma_{E_j}}}\right)\\&\quad\times f(\gamma_{M_j})d\gamma_{M_j}\\&=\mathbf{E}\left[\ln(1+\gamma_{M_j})\mathbf{\Phi}\left(\frac{\ln\gamma_{M_j}-\mu_{\gamma_{E_j}}}{\sigma_{\gamma_{E_j}}}\right)\right],\end{aligned} \tag{12}$$

and

$$\begin{aligned}\bar{\mathbf{C}}'_{E_j}(\gamma_{E_j})&=\int_0^\infty\ln(1+\gamma_{E_j})\mathbf{Q}\left(\frac{\ln\gamma_{E_j}-\mu_{\gamma_{M_j}}}{\sigma_{\gamma_{M_j}}}\right)\\&\quad\times f(\gamma_{E_j})d\gamma_{E_j}\\&=\mathbf{E}\left[\ln(1+\gamma_{E_j})\mathbf{Q}\left(\frac{\ln\gamma_{E_j}-\mu_{\gamma_{M_j}}}{\sigma_{\gamma_{M_j}}}\right)\right],\end{aligned} \tag{13}$$

where $j\in\{1,2\}$, $\mathbf{\Phi}(\cdot)$ denotes the cumulative distribution function (CDF) of standard normal distribution and $\mathbf{Q}(Z)=1/\sqrt{2\pi}\int_Z^\infty\exp(-t^2/2)dt$. Thus, by using (9), (12), and (13), the difference terms in (11) can be simplified as

$$\begin{aligned}\left[\bar{\mathbf{C}}'_{M_j}(\gamma_{M_j})-\bar{\mathbf{C}}'_{E_j}(\gamma_{E_j})\right]&\approx\frac{2}{3}\left[\psi_{M_j}\left(\mu_{\gamma_{M_j}}\right)-\psi_{E_j}\left(\mu_{\gamma_{E_j}}\right)\right]\\&\quad+\frac{1}{6}\left[\psi_{M_j}\left(\mu_{\gamma_{M_j}}+\sqrt{3}\sigma_{\gamma_{M_j}}\right)-\psi_{E_j}\left(\mu_{\gamma_{E_j}}+\sqrt{3}\sigma_{\gamma_{E_j}}\right)\right]\\&\quad+\frac{1}{6}\left[\psi_{M_j}\left(\mu_{\gamma_{M_j}}-\sqrt{3}\sigma_{\gamma_{M_j}}\right)-\psi_{E_j}\left(\mu_{\gamma_{E_j}}-\sqrt{3}\sigma_{\gamma_{E_j}}\right)\right],\end{aligned} \tag{14}$$

where $\psi_{M_j}(y)=\ln(1+\exp(y))\mathbf{\Phi}((y-\mu_{\gamma_{E_j}})/\sigma_{\gamma_{E_j}})$, $\psi_{E_j}(y)=\ln(1+\exp(y))\mathbf{Q}((y-\mu_{\gamma_{M_j}})/\sigma_{\gamma_{M_j}})$, and $j\in\{1,2\}$. On substituting (14) into (11), we obtain the desired analytical ASC of the considered PLC system.

2) *Case-II, Correlated main and wiretap PLC channel:* The analytical ASC of the correlated PLC system is derived as

$$\begin{aligned}\bar{\mathbf{C}}_{\mathbf{s}}(\gamma_M,\gamma_E)&=(1-p)\times\mathbf{E}\left[\mathbf{C_s}(\gamma_{M_1},\gamma_{E_1})\right]\\&\quad+p\times\mathbf{E}\left[\mathbf{C_s}(\gamma_{M_2},\gamma_{E_2})\right]\\&=(1-p)\times\left[\int_0^\infty\ln(1+\gamma_{M_1})\int_0^{\gamma_{M_1}}f_{\gamma_{M_1},\gamma_{E_1}}(\gamma_{M_1},\gamma_{E_1})d\gamma_{E_1}d\gamma_{M_1}\right.\\&\quad\left.-\int_0^\infty\ln(1+\gamma_{E_1})\int_{\gamma_{E_1}}^\infty f_{\gamma_{M_1}\gamma_{E_1}}(\gamma_{M_1},\gamma_{E_1})d\gamma_{M_1}d\gamma_{E_1}\right]\\&\quad+p\times\left[\int_0^\infty\ln(1+\gamma_{M_2})\int_0^{\gamma_{M_2}}f_{\gamma_{M_2},\gamma_{E_2}}(\gamma_{M_2},\gamma_{E_2})d\gamma_{E_2}d\gamma_{M_2}\right.\\&\quad\left.-\int_0^\infty\ln(1+\gamma_{E_2})\int_{\gamma_{E_2}}^\infty f_{\gamma_{M_2}\gamma_{E_2}}(\gamma_{M_2},\gamma_{E_2})d\gamma_{M_2}d\gamma_{E_2}\right]\\&=(1-p)\times\left[Z_{X_1}-Z_{Y_1}\right]+p\times\left[Z_{X_2}-Z_{Y_2}\right].\end{aligned} \tag{15}$$

Eq. (15) is derived by using [15, Eq. (11)]. Further, in (15),

$$Z_{X_j} \approx \frac{2}{3}\psi_{Z_{X_j}}\left(\mu_{\gamma_{M_j}}\right) + \frac{1}{6}\psi_{Z_{X_j}}\left(\mu_{\gamma_{M_j}} + \sqrt{3}\sigma_{\gamma_{M_j}}\right) + \frac{1}{6}\psi_{Z_{X_j}}\left(\mu_{\gamma_{M_j}} - \sqrt{3}\sigma_{\gamma_{M_j}}\right), j \in \{1,2\}, \quad (16)$$

$$Z_{Y_j} \approx \frac{2}{3}\psi_{Z_{Y_j}}\left(\mu_{\gamma_{E_j}}\right) + \frac{1}{6}\psi_{Z_{Y_j}}\left(\mu_{\gamma_{E_j}} + \sqrt{3}\sigma_{\gamma_{E_j}}\right) + \frac{1}{6}\psi_{Z_{Y_j}}\left(\mu_{\gamma_{E_j}} - \sqrt{3}\sigma_{\gamma_{E_j}}\right), j \in \{1,2\}, \quad (17)$$

where

$$\psi_{Z_{X_j}}(x) = \ln\left(1+\exp(x)\right)\mathbf{\Phi}\left(\frac{x-\mu_{\gamma_{E_j}} - \rho\frac{\sigma_{\gamma_{E_j}}}{\sigma_{\gamma_{M_j}}}\left(x-\mu_{\gamma_{M_j}}\right)}{\sqrt{(1-\rho^2)}\sigma_{\gamma_{E_j}}}\right)$$

$$\psi_{Z_{Y_j}}(x) = \ln\left(1+\exp(x)\right)\mathbf{Q}\left(\frac{x-\mu_{\gamma_{M_j}} - \rho\frac{\sigma_{\gamma_{M_j}}}{\sigma_{\gamma_{E_j}}}\left(x-\mu_{\gamma_{E_j}}\right)}{\sqrt{(1-\rho^2)}\sigma_{\gamma_{M_j}}}\right).$$

Here, ρ denotes correlation coefficient. Thus, by substituting (16) and (17) into (15), we achieve the desired expression of ASC for the considered correlated PLC system.

C. Computation of SOP

SOP is that probability when the instantaneous secrecy capacity is less than a given threshold secrecy capacity ($\mathbf{C}_{\rm th}$) [15], [16].

1) *Case-I, Independent main and wiretap PLC channel:* The SOP of the considered PLC system is expressed as

$$\begin{aligned} P_{\rm out} &= (1-p)\times\left[\Pr\left\{\mathbf{C_s}(\gamma_{M_1},\gamma_{E_1}) < \mathbf{C}_{\rm th}\right\}\right] \\ &\quad + p\times\left[\Pr\left\{\mathbf{C_s}(\gamma_{M_2},\gamma_{E_2}) < \mathbf{C}_{\rm th}\right\}\right], \\ &= (1-p)\times\left[\Pr\left\{\frac{1+\gamma_{M_1}}{1+\gamma_{E_1}} < \exp(\mathbf{C}_{\rm th})\right\}\right] \\ &\quad + p\times\left[\Pr\left\{\frac{1+\gamma_{M_2}}{1+\gamma_{E_2}} < \exp(\mathbf{C}_{\rm th})\right\}\right], \\ &= (1-p)\times\left[\Pr\{\gamma_{M_1} < \beta\gamma_{E_1}+\beta-1\}\right] \\ &\quad + p\times\left[\Pr\{\gamma_{M_2} < \beta\gamma_{E_2}+\beta-1\}\right], \end{aligned} \quad (18)$$

where $\beta = \exp(\mathbf{C}_{\rm th})$. After some mathematical manipulations, (18) can be re-written as

$$P_{\rm out} = (1-p)\times\left[1-\bar{\mathbf{P}}'_{E_1}(\gamma_{E_1})\right] + p\times\left[1-\bar{\mathbf{P}}'_{E_2}(\gamma_{E_2})\right], \quad (19)$$

where

$$\begin{aligned} \bar{\mathbf{P}}'_{E_j}(\gamma_{E_j}) &= \int_0^\infty f(\gamma_{E_j})\mathbf{Q}\left(\frac{\ln(\beta\gamma_{E_j}+\beta-1)-\mu_{\gamma_{M_j}}}{\sigma_{\gamma_{M_j}}}\right)d\gamma_{E_j} \\ &= \mathbf{E}\left[\mathbf{Q}\left(\frac{\ln(\beta\gamma_{E_j}+\beta-1)-\mu_{\gamma_{M_j}}}{\sigma_{\gamma_{M_j}}}\right)\right]. \end{aligned} \quad (20)$$

In (20), $j \in \{1,2\}$. Now, utilizing (9), $\bar{\mathbf{P}}'_{E_j}(\gamma_{E_j})$ is solved as

$$\begin{aligned} &\bar{\mathbf{P}}'_{E_j}(\gamma_{E_j}) \\ &\approx \frac{2}{3}\mathbf{Q}\left(\frac{\Omega\left(\mu_{\gamma_{E_j}}\right)-\mu_{\gamma_{M_j}}}{\sigma_{\gamma_{M_j}}}\right) - \frac{1}{6}\mathbf{Q}\left(\frac{\Omega\left(\mu_{\gamma_{E_j}}+\sqrt{3}\sigma_{\gamma_{E_j}}\right)-\mu_{\gamma_{M_j}}}{\sigma_{\gamma_{M_j}}}\right) \\ &\quad - \frac{1}{6}\mathbf{Q}\left(\frac{\Omega\left(\mu_{\gamma_{E_j}}-\sqrt{3}\sigma_{\gamma_{E_j}}\right)-\mu_{\gamma_{M_j}}}{\sigma_{\gamma_{M_j}}}\right), \end{aligned} \quad (21)$$

where $j \in \{1,2\}$ and $\Omega(x) = \ln(\beta\exp(x)+\beta-1)$. As a result, the analytical SOP is obtained by substituting (21) into (19).

2) *Case-II, Correlated main and wiretap PLC channel:* Using [15, Eq. (31)], the analytical SOP for correlated PLC system is calculated as

$$P_{\rm out} = (1-p)\times[\bar{\mathbf{P}}'_{E_1}(\gamma_{E_1})] + p\times[\bar{\mathbf{P}}'_{E_2}(\gamma_{E_2})], \quad (22)$$

where

$$\bar{\mathbf{P}}'_{E_j}(\gamma_{E_j}) \approx \frac{1}{6}\left[4\Xi\left(\mu_{\gamma_{E_j}}\right) + \Xi\left(\mu_{\gamma_{E_j}}+\sqrt{3}\sigma_{\gamma_{E_j}}\right) + \Xi\left(\mu_{\gamma_{E_j}}-\sqrt{3}\sigma_{\gamma_{E_j}}\right)\right], j \in \{1,2\}. \quad (23)$$

In Eq. (23),

$$\Xi(\mu_{\gamma_{E_j}}) = \frac{1}{2}\left[1+\mathrm{erf}\left(\frac{\psi(\gamma_{E_j}) - \rho\frac{\ln(\mu_{\gamma_{E_j}})-\mu_{\gamma_{E_j}}}{\sqrt{2}\sigma_{\gamma_{E_j}}}}{\sqrt{1-\rho^2}}\right)\right]$$

$$\psi(\gamma_{E_j}) = \frac{\ln(\beta\gamma_{E_j}+\beta-1)-\mu_{\gamma_{M_j}}}{\sqrt{2}\sigma_{\gamma_{M_j}}}, j \in \{1,2\}.$$

Now, substituting (23) into (22) desired analytical expression of correlated SOP is achieved.

D. Computation of SPSC

The SPSC is defined as the probability of existence of secrecy capacity and serves as a fundamental benchmark for secrecy performance. The analytical SPSC of the considered PLC system is, thus, given by [15], [16]

$$\begin{aligned} SPSC &= \Pr\{\mathbf{C_s}(\gamma_D,\gamma_E) > 0\} \\ &= (1-p)\times\Pr\{\gamma_{M_1} > \gamma_{E_1}\} \\ &\quad + p\times\Pr\{\gamma_{M_2} > \gamma_{E_2}\} \\ &= (1-p)\times\left[1-\Pr\{\gamma_{M_1} < \gamma_{E_1}\}\right] \\ &\quad + p\times\left[1-\Pr\{\gamma_{M_2} < \gamma_{E_2}\}\right]. \end{aligned} \quad (24)$$

In (25),

$$\begin{aligned} \Pr\{\gamma_{M_j} < \gamma_{E_j}\} &= \int_0^\infty f(\gamma_{M_j})\mathbf{Q}\left(\frac{\ln\gamma_{M_j}-\mu_{\gamma_{E_j}}}{\sigma_{\gamma_{E_j}}}\right)d\gamma_{M_j} \\ &= \mathbf{E}\left[\mathbf{Q}\left(\frac{\ln\gamma_{M_j}-\mu_{\gamma_{E_j}}}{\sigma_{\gamma_{E_j}}}\right)d\gamma_{M_j}\right], \end{aligned} \quad (25)$$

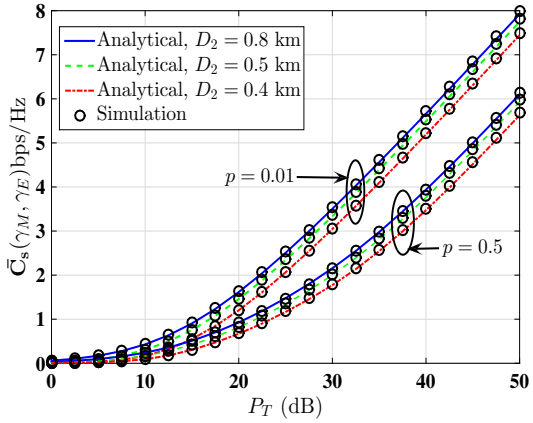

Fig. 2. Comparison of ASC vs P_T for various values of D_2 when $p = 0.01, 0.5$, $D_1 = 0.4$ km, and $P_L = 50$ dB/km.

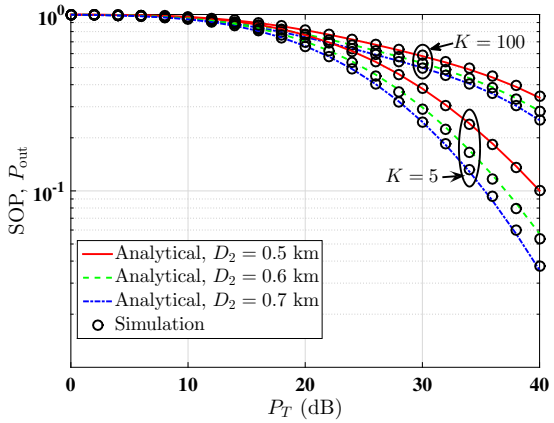

Fig. 3. Comparison of SOP vs P_T for various values of D_2 when $K = 5, 100$, $p = 0.01$, $D_1 = 0.5$ km, and $P_L = 50$ dB/km.

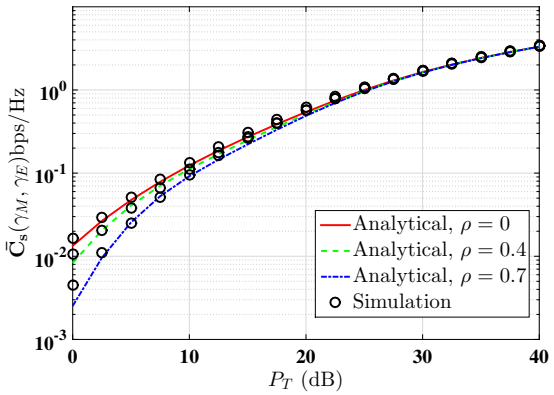

Fig. 4. Comparison of ASC vs P_T for various values of ρ when $p = 0.2$, $D_1 = D_2 = 0.6$ km, and $P_L = 50$ dB/km.

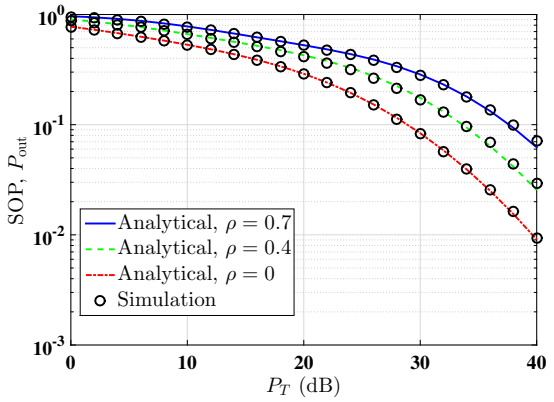

Fig. 5. Comparison of SOP vs P_T for various values of ρ when $K = 100$, $D_1 = D_1 = 0.5$ km, and $P_L = 50$ dB/km.

where $j \in \{1,2\}$. Now, using (9), Eq. (25) is evaluated as

$$\begin{aligned}\Pr\{\gamma_{M_j} < \gamma_{E_j}\} &\approx \frac{2}{3}\mathbf{Q}\left(\frac{\mu_{\gamma_{M_j}} - \mu_{\gamma_{E_j}}}{\sigma_{\gamma_{E_j}}}\right) - \frac{1}{6}\mathbf{Q}\left(\frac{\mu_{\gamma_{M_j}} + \sqrt{3}\sigma_{\gamma_{M_j}} - \mu_{\gamma_{E_j}}}{\sigma_{\gamma_{E_j}}}\right) \\ &\quad - \frac{1}{6}\mathbf{Q}\left(\frac{\mu_{\gamma_{M_j}} - \sqrt{3}\sigma_{\gamma_{M_j}} - \mu_{\gamma_{E_j}}}{\sigma_{\gamma_{E_j}}}\right), j \in \{1,2\}. \end{aligned} \tag{26}$$

As a result, the analytical SPSC of the considered PLC system is obtained by substituting (26) into (24).

TABLE I
PARAMETER VALUES USED FOR SIMULATIONS.

No.	Parameter	Value
1	σ_{γ_k}	2
2	μ_{h_k}	1
3	$\mathbf{C}_{\text{th}}$	1
4	D_1	0.4 km, 0.5 km
5	D_2	0.4 km, 0.5 km, 0.8 km
6	N	10^5 Samples
7	P_L	50 dB/km

IV. Numerical Results and Discussion

In this section, we present the analytical and simulation results for the considered PLC system. The parameter values used for the simulations are mentioned in TABLE I.

Fig. 2 shows a comparison of ASC of the considered PLC system as a function of $P_T(dB)$ for various values of Eve distance (D_2), when $p = 0.01$ and 0.5. We assume that Bob (M) is located at a fixed distance $D_1 = 0.5$ km from Alice (A) with $P_L = 50$ dB/km, and transmitted power on A to (E) link is fixed at 10 dB. It can be observed from the figure that ASC increases with increase in Eve distance (D_2) from 0.5 km to 0.8 km. This is due to the fact that with the increasing distance, the SNR at the eavesdropper becomes poor. We also note that as the arrival probability of impulsive noise samples (p) varies from 0.01 to 0.5, the ASC deteriorates. The impact of impulsive noise component on ASC is more dominating at lower Eve distances for high values of p. The simulation results closely match with the analytical results,

thereby establishing the validity of the derived expressions.

Fig. 3 presents the analytical and simulation results of SOP versus transmitted power, (P_T), for various values of Eve distance (D_2), when $K = 5$ and 100. It is assumed that Bob (M) is located at a fixed distance $D_1 = 0.5$ km from Alice (A) with transmitted power on A to (E) link fixed at 10 dB, and $P_L = 50$ dB/km. It can be noticed from the figure that the SOP falls with the increasing P_T. Further, the SOP takes higher values for high value of K and decreases for lower values of K signifying SOP of the system increases as the power of the impulsive noise increases compared to the power of the background noise. The analytical SOP curves are plotted using (19).

Fig. 4 represents the analytical and simulation results of ASC versus transmitted power (P_T), when both main and wiretap channels correlated log-normal channels. The plots are obtained for different values of ρ with fixed distances, $D_1 = D_2$= 0.5 km, $K = 100$, $P_L = 50$ dB/km, and $p = 0.4$. The computational ASC curves are plotted using (15). It can be observed that ASC decreases with a higher value of ρ and vice-versa, which shows a stronger correlation between the channels deteriorates the ASC performance. The impact of impulsive noise component remains the same as previous results.

In Fig. 5, we plot the SOP as a function of P_T, when both main and wiretap channels are correlated log-normal channels. The curves are plotted for different values of ρ with fixed distances, $D_1 = D_2$= 0.5 km, $K = 100$, $P_L = 50$ dB/km, and $p = 0.4$. The numerical plots are obtained using (22). The figure indicates that the SOP is higher for higher values of ρ, thereby revealing that stronger correlation between the channels leads to poorer SOP.

The analytical and simulation results of SPSC as a function of P_T for different values of p and K is exhibited in Fig. 6 with transmitted power on A to (E) link fixed at 10 dB, $D_1 = D_2 = 0.5$ km, and $P_L = 50$ dB/km. The computational curves are obtained using (24). It can be noticed from the figure that the SPSC increases with increase in transmitted power. We also observe that as the arrival probability of the impulsive noise increases, SPSC becomes poor. The adverse effect of parameter K on SPSC is also evident from the figure as for higher value of K SPSC deteriorates, while keeping p fixed.

V. CONCLUSION

In this paper, we have analyzed PLS of the power line wiretap channel model in the presence of a passive eavesdropper. The approximate analytical closed-form expressions have been established in terms of ASC, SOP, and SPSC for independent and correlated channels. Further, the MATLAB platform is used to validate the numerical results by the Monte Carlo simulation method. Useful insights into the secrecy performance are obtained through the numerical results.

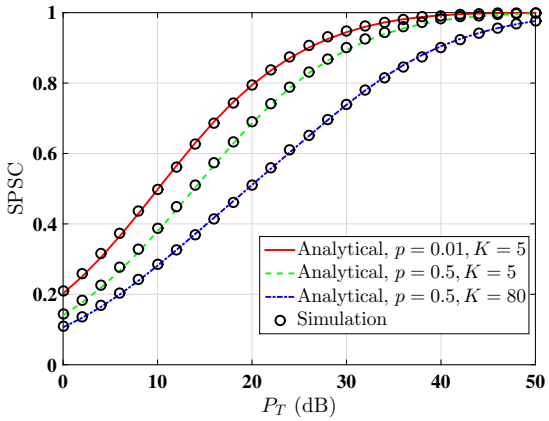

Fig. 6. Comparison of SPSC vs P_T for various values of K when $D_1 = D_2 = 0.5$ km, $p = 0.01, 0.5$, and $P_L = 50$ dB/km.

REFERENCES

[1] L. d. M. B. A. Dib, V. Fernandes, M. de L. Filomeno, and M. V. Ribeiro, "Hybrid PLC/wireless communication for smart grids and internet of things applications," *Internet Things J.*, vol. 5, no. 2, pp. 655–667, Apr. 2018.

[2] S. Baig, H. Muhammad Asif, T. Umer, S. Mumtaz, M. Shafiq, and J. Choi, "High data rate discrete wavelet transform-based PLC-VLC design for 5g communication systems," *IEEE Access*, vol. 6, pp. 52 490–52 499, Sept. 2018.

[3] A. Pittolo and A. M. Tonello, "Physical layer security in power line communication networks: an emerging scenario, other than wireless," *IET Commun.*, vol. 8, no. 8, pp. 1239–1247, May 2014.

[4] A. Salem, K. A. Hamdi, and E. Alsusa, "Physical layer security over correlated log-normal cooperative power line communication channels," *IEEE Access*, vol. 5, pp. 13 909–13 921, Jul. 2017.

[5] Y. Zhuang and L. Lampe, "Physical layer security in mimo power line communication networks," in *18th IEEE Int. Symp. Power Line Commun. Appl.*, Mar. 2014, pp. 272–277.

[6] A. Mathur, M. R. Bhatnagar, and B. K. Panigrahi, "PLC performance evaluation with channel gain and additive noise over nonuniform background noise phase," *Wiley Trans. Emerg. Telecommun. Technol.*, vol. 28, no. 5, p. e3131, May 2017.

[7] A. Dubey and R. K. Mallik, "PLC system performance with AF relaying," *IEEE Trans. Commun.*, vol. 63, no. 6, pp. 2337–2345, Jun. 2015.

[8] A. Dubey, D. Sharma, R. K. Mallik, and S. Mishra, "Modeling and performance analysis of a PLC system in presence of impulsive noise," in *2015 IEEE Power Energy Soc. General Meeting*, Jul. 2015, pp. 1–5.

[9] L. Lutz and A. Han Vinck, "On cooperative coding for narrow band PLC networks," *AEU-Int. J. Electron. and Commun.*, vol. 65, no. 8, pp. 681–687, 2011.

[10] G. Hooijen, "On the channel capacity of the residential power circuit used as a digital communications medium," *IEEE Commun. Lett.*, vol. 2, no. 10, pp. 267–268, 1998.

[11] A. Mathur, M. R. Bhatnagar, and B. K. Panigrahi, "Performance evaluation of PLC under the combined effect of background and impulsive noises," *IEEE Commun. Lett.*, vol. 19, no. 7, pp. 1117–1120, Jul. 2015.

[12] G. Kaddoum and N. Tadayon, "Differential chaos shift keying: A robust modulation scheme for power-line communications," *IEEE Trans. Circuits Syst. II, Exp. Briefs*, vol. 64, no. 1, pp. 31–35, Jan. 2017.

[13] A. Mathur, M. R. Bhatnagar, Y. Ai, and M. Cheffena, "Performance analysis of a dual-hop wireless-power line mixed cooperative system," *IEEE Access*, vol. 6, pp. 34 380–34 392, Jun. 2018.

[14] J. M. Holtzman, "A simple, accurate method to calculate spread-spectrum multiple-access error probabilities," *IEEE Trans. Commun.*, vol. 40, no. 3, pp. 461–464, Mar. 1992.

[15] G. Pan, C. Tang, X. Zhang, T. Li, Y. Weng, and Y. Chen, "Physical-layer security over non-small-scale fading channels," *IEEE Trans. Veh. Technol.*, vol. 65, no. 3, pp. 1326–1339, Mar. 2016.

[16] M. Bloch, J. Barros, M. R. D. Rodrigues, and S. W. McLaughlin, "Wireless information-theoretic security," *IEEE Trans. Inf. Theory*, vol. 54, no. 6, pp. 2515–2534, Jun. 2008.